

Dynamical and Thermal Problems in Vortex Development and Movement. Part I: A PV–Q View

ZHENG Yongjun^{1,2} (郑永骏), WU Guoxiong^{1*} (吴国雄), and LIU Yimin¹ (刘屹岷)

¹ State Key Laboratory of Numerical Modeling for Atmospheric Sciences and Geophysical Fluid Dynamics, Institute of Atmospheric Physics, Chinese Academy of Sciences, Beijing 100029

² Graduate University of the Chinese Academy of Sciences, Beijing 100049

(Received March 28, 2012; in final form June 18, 2012)

ABSTRACT

Based on the Lagrangian change equation of vertical vorticity deduced from the equation of three-dimensional Ertel potential vorticity (PV_e), the development and movement of vortex are investigated from the view of potential vorticity and diabatic heating (PV–Q). It is demonstrated that the asymmetric distribution in the vortex of the non-uniform diabatic heating in both vertical and horizontal can lead to the vortex's development and movement. The theoretical results are used to analyze the development and movement of a Tibetan Plateau (TP) vortex (TPV), which appeared over the TP, then slid down and moved eastward in late July 2008, resulting in heavy rainfall in Sichuan Province and along the middle and lower reaches of the Yangtze River. The relative contributions to the vertical vorticity development of the TPV are decomposed into three parts: the diabatic heating, the change in horizontal component of PV_e (defined as PV_2), and the change in static stability θ_z . The results show that in most cases, diabatic heating plays a leading role, followed by the change in PV_2 , while the change of θ_z usually has a negative impact in a stable atmosphere when the atmosphere becomes more stable, and has a positive contribution when the atmosphere approaches neutral stratification. The intensification of the TPV from 0600 to 1200 UTC 22 July 2008 is mainly due to the diabatic heating associated with the precipitation on the eastern side of the TPV when it uplifted on the up-slope of the northeastern edge of the Sichuan basin. The vertical gradient of diabatic heating makes positive (negative) PV_e generation below (above) the maximum of diabatic heating; the positive PV_e generation not only intensifies the low-level vortex but also enhances the vertical extent of the vortex as it uplifts. The change in PV_e due to the horizontal gradient of diabatic heating depends on the vertical shear of horizontal wind that passes through the center of diabatic heating. The horizontal gradient of diabatic heating makes positive (negative) PV_e generation on the right (left) side of the vertical shear of horizontal wind. The positive PV_e generation on the right side of the vertical shear of horizontal wind not only intensifies the local vertical vorticity but also affects direction of movement of the TPV. These diagnostic results are in good agreement with the theoretic results developed from the PV–Q view.

Key words: Tibetan Plateau vortex, vorticity development, potential vorticity, diabatic heating, Lagrangian change

Citation: Zheng Yongjun, Wu Guoxiong, and Liu Yimin, 2013: Dynamical and thermal problems in vortex development and movement. Part I: A PV–Q view. *Acta Meteor. Sinica*, **27**(1), 1–14, doi: 10.1007/s13351-013-0101-3.

1. Introduction

In a frictionless and adiabatic dry atmosphere, the Ertel potential vorticity (PV_e) is conserved (Ertel, 1942). The application of the Ertel potential vorticity in the diagnosis of atmospheric motion has been summarized by Hoskins et al. (1985). Based on the conservation of Ertel potential vorticity, Wu and Liu

(1997) proposed a theory of slantwise vorticity development (SVD) to interpret the development of vertical vorticity of a Lagrangian particle which is sliding down a slantwise isentropic surface. Many applications of the SVD theory have obtained reasonable results and demonstrated the development of vertical vorticity on the slope of isentropic surface (Cui et al., 2002; Ma et al., 2002; Chen et al., 2004; Jiang et al., 2004;

Supported by the National Basic Research and Development (973) Program of China (2012CB417203 and 2010CB950403) and National Natural Science Foundation of China (40875034 and 40925015).

*Corresponding author: gxwu@lasg.iap.ac.cn.

Chinese version to be published.

©The Chinese Meteorological Society and Springer-Verlag Berlin Heidelberg 2013

Wang et al., 2007). However, the vertical vorticity development depends not only on C_D , but also on static stability θ_z under the conservation of PV_e . More importantly, the latent heat release associated with precipitation plays a significant role in the vertical vorticity development (Shen et al., 1986; Ding and Lu, 1990; Chen et al., 1996). Therefore, to understand how diabatic heating contributes to the vertical vorticity development from the view of potential vorticity and diabatic heating (PV-Q) becomes important, and is one of the subjects of this study.

The Tibetan Plateau (TP) vortex (TPV) is a shallow low-level cyclonic system near 500 hPa over the TP and in the lower troposphere over the plain areas. The TPV is common in boreal summer. In general, it originates over the central-western TP, moves eastward, and dies out over the eastern TP. Its horizontal and vertical scales are typically about 500 and 2–3 km, respectively. Sometimes, the TPV moves eastward out of the TP, and often results in severe weather over eastern China, especially over the Sichuan basin (Ye and Gao, 1979; Tao and Ding, 1981; Qiao and Zhang, 1994; Li, 2002). Previous studies have depicted that the formation of the TPV is due to surface sensible heating, topography, static stability, friction of boundary layer, and large-scale circulation of the midlatitude trough or cyclone (Tao, 1980; Group of Tibetan Plateau Low Value System, 1978; Zhang et al., 1988; Ding, 1993, 2005; Chen et al., 1996). It is generally believed that the development of the TPV is closely related to the diabatic heating especially the condensation heat release (Shen et al., 1986; Ding and Lu, 1990; Chen et al., 1996). The movement of the TPV depends on the difference of divergence between 200 and 500 hPa (Liu and Fu, 1985) and the steering flow of the southwesterly jet at 300 hPa (Qiao, 1987; Sun and Chen, 1988). But how does the three-dimensional heterogeneous distribution of the diabatic heating affect the development and movement of the TPV? What is the relationship between diabatic heating and circulation configuration during the development of the TPV? These are still unclear and need to be investigated. An attempt to understand these questions by employing the theory of vertical vorticity development is another subject of this study.

This paper is organized as follows. In Section 2, a brief description of a TPV case in July 2008 and its background circulation are given. The Lagrangian approach of the vertical vorticity development in terms of the three-dimensional diabatic heating, atmospheric circulation, and thermal structure is investigated from the view of potential vorticity and diabatic heating (PV-Q) in Section 3. Their relative contributions to the vertical vorticity development of the changes in PV_e , the horizontal component of Ertel potential vorticity (PV_2), and the static stability θ_z , especially the influence of non-uniform structure of diabatic heating in vertical and horizontal directions on the intensification of vertical vorticity and the movement of the vortex, are demonstrated by employing the theory to the TPV case in Section 4. Finally, conclusions and discussion are summarized in Section 5.

2. Description of the TPV in July 2008

The data used in this study are the ERA-Interim reanalysis data with a horizontal resolution of 0.75° (Dee et al., 2011) and the TRMM 3B42 precipitation data with a 3-h interval and a 0.25° horizontal resolution (Huffman et al., 2007). The ERA-Interim reanalysis data have 60 hybrid levels in the vertical with the top level at 0.1 hPa, and 4 times per day at 0000, 0600, 1200, and 1800 UTC since 1979. All the computations in this study are performed at the model level with vertical coordinates transformed so that the vertical and horizontal components of vorticity and gradient are strictly perpendicular and acyclic, respectively. In addition, the results are interpolated onto the isobaric or isentropic surfaces for easy plotting of the figures.

2.1 Track of the TPV and associated precipitation

In late July 2008, a TPV formed over the western TP (figure omitted) and moved eastward over the eastern TP on 20 July 2008 (Fig. 1). Then, it moved out of the TP after 1800 UCT 20 July 2008 and shifted southward suddenly at 1200 UTC 21 July 2008. Finally, it moved east-northeastward from 22 July 2008 and died out over the Yellow Sea on 23 July 2008. The track of the TPV and the horizontal pattern of associated 6-h accumulated precipitation are

shown in Fig. 1, and the time series of the central maximum vertical relative vorticity of the TPV and the $3^\circ \times 3^\circ$ area average of every 6-h precipitation around the center of the TPV are shown in Fig. 2. As the TPV moved eastward from 1800 UTC 20 July 2008 onward, it generated heavy rainfall over the eastern China to its east, especially over the Sichuan basin,

Hubei, Anhui, Henan, and Shandong provinces. As shown in Fig. 2, the central vertical relative vorticity intensified at 1800 UTC 20 July 2008 when the TPV just started to move down the TP. On 21 July 2008, the TPV was located at the Sichuan basin, the vertical relative vorticity decreased, but the precipitation over the center and east of the Sichuan basin increased

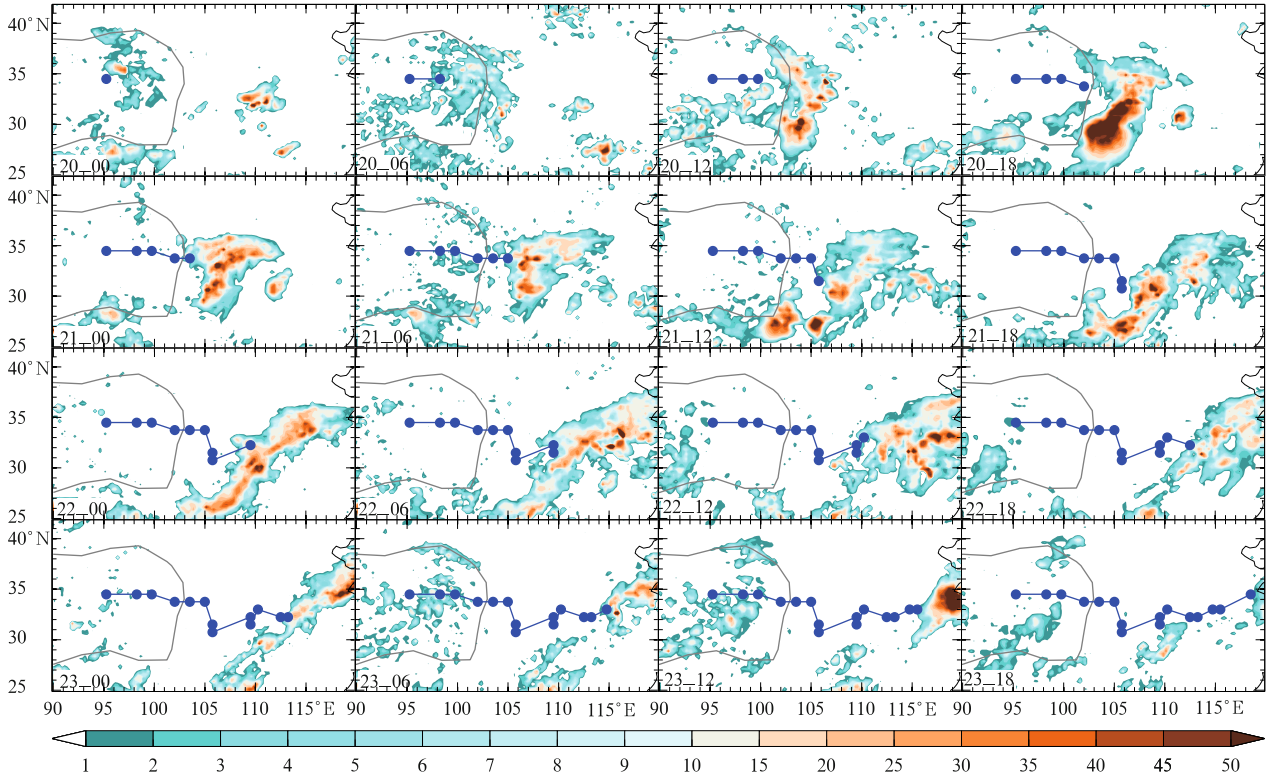


Fig. 1. Track of the TPV from 0000 UTC 20 to 1800 UTC 23 July 2008 and the associated 6-h precipitation. Shading represents the TRMM 3B42 precipitation (mm (6 h)^{-1}) and blue curve with solid circle indicates the track of the TPV. The thick gray solid curve indicates the 3000-m contour of the terrain height, and the label dd-hh denotes hh UTC dd July 2008, the same for following figures.

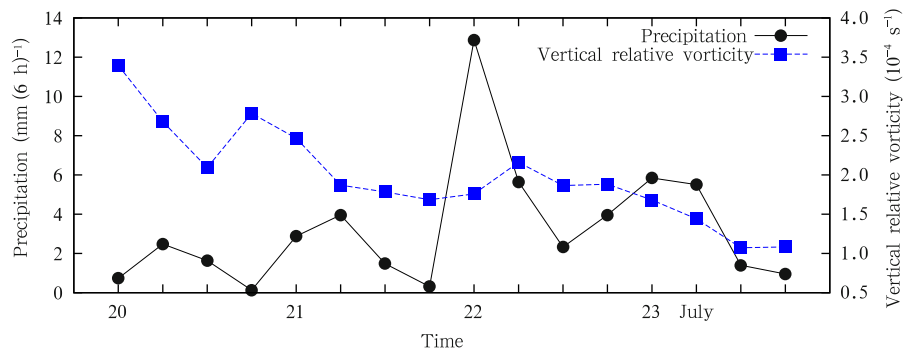


Fig. 2. Time series of the central maximum vertical relative vorticity (dashed line; 10^{-4} s^{-1}) of the TPV and the $3^\circ \times 3^\circ$ area average of associated precipitation (solid line; mm (6 h)^{-1}) around the center of the TPV from 0000 UTC 20 to 1800 UTC 23 July 2008.

tremendously. The period from 0000 UTC 20 to 1800 UTC 21 July 2008 is defined as the first stage of the TPV development, during which it slid downward from the TP to the Sichuan basin and triggered severe rainfall over Sichuan Province. The second stage of the TPV is from 0000 UTC 22 to 1800 UTC 23 July 2008, during which the TPV moved northeastward and produced heavy rainfall over Hubei, Anhui, Henan, and Shandong provinces. In this stage, the vertical vorticity restrengthened at 0600 UTC 22 July 2008, and then weakened gradually. But the intensification of precipitation was at 0000 UTC 22 July 2008, ahead of the intensification of vertical vorticity (Fig. 2). This phenomenon implies that the vertical vorticity intensification may be due to diabatic heating associated with the precipitation, which will be discussed further in Section 4.

2.2 Large-scale circulation associated with the TPV

Distributions of the 300- and 500-hPa horizontal wind, geopotential height, and vertical relative vorticity at 0600 and 1800 UTC 20 July 2008 are presented in Figs. 3a and 3b, respectively. These figures demonstrate the circulations associated with the TPV before it moved down off the TP. At 0600 UTC 20 July 2008 (Fig. 3a) at 300 hPa in midlatitudes, a weak geopotential height ridge was located near 100°E, and a trough was over northern China. Along the subtropics, westerly prevailed, with a weak trough over the northeastern TP. At 500 hPa, the trough was near the TP surface and the circulation pattern was similar to that at 300 hPa; however, the trough over the northeastern TP was strong. A strong closed cyclone with vorticity of more than 10^{-4} s^{-1} was embedded in the trough, which is the TPV under the current study. At 1800 UTC (Fig. 3b), the general feature of the circulation did not change much except an eastward shifting. Consequently, the eastern portion of the TPV had slid down the eastern slope of the TP, while the vorticity center was still over the eastern TP. Figures 3c and 3d are the same as Figs. 3a and 3b except for 500 and 700 hPa at 0600 and 1200 UTC 22 July 2008, respectively. These present the circulations associated with the vortex during its second stage. The circulation was featured with high geopotential to the west of 100°E and low geopotential to its

east. As the TPV moved eastward, the closed cyclone slid down to the lower troposphere, and evolved to a developing vortex at 700 hPa and an eastward moving midlatitude trough at 500 hPa. As described above, the TPV reintensified at 0600 UTC 22 July 2008 (Fig. 3c), and reached 500 hPa where the closed contour of 580 dgpm was re-established at 1200 UTC 22 July 2008 (Fig. 3d).

3. PV-Q view on vertical vorticity development

By definition, PV_e (Ertel, 1942) is expressed as

$$PV_e = \alpha(2\Omega + \nabla \times \mathbf{V}) \cdot \nabla\theta = \boldsymbol{\eta}_a \cdot \nabla\theta, \quad (1)$$

where $\boldsymbol{\eta}_a = \eta_x \mathbf{i} + \eta_y \mathbf{j} + \eta_z \mathbf{k}$ is the absolute vorticity per unit mass, and $\nabla = \frac{\partial}{\partial x} \mathbf{i} + \frac{\partial}{\partial y} \mathbf{j} + \frac{\partial}{\partial z} \mathbf{k}$ is three-dimensional gradient operator. Define the horizontal component of PV_e as

$$PV_2 = \eta_x \theta_x + \eta_y \theta_y = \boldsymbol{\eta}_s \cdot \boldsymbol{\theta}_s, \quad (2)$$

where $\boldsymbol{\eta}_s = \eta_x \mathbf{i} + \eta_y \mathbf{j}$ is horizontal vorticity, $\boldsymbol{\theta}_s = \theta_x \mathbf{i} + \theta_y \mathbf{j} = \nabla_s \theta$ is horizontal gradient of potential temperature, and $\nabla_s = \frac{\partial}{\partial x} \mathbf{i} + \frac{\partial}{\partial y} \mathbf{j}$ is horizontal gradient operator. Then

$$\eta_z = \frac{PV_e - PV_2}{\theta_z} = \frac{PV_e}{\theta_z} - C_D, \quad \theta_z \neq 0, \quad (3)$$

where

$$C_D = \frac{PV_2}{\theta_z} = \frac{\boldsymbol{\eta}_s \cdot \boldsymbol{\theta}_s}{\theta_z}, \quad \theta_z \neq 0. \quad (4)$$

The notations used here are as following: $\eta_x = \alpha \left(\frac{\partial w}{\partial y} - \frac{\partial v}{\partial z} \right)$, $\eta_y = \alpha \left(e + \frac{\partial u}{\partial z} - \frac{\partial w}{\partial x} \right)$, $\eta_z = \alpha \left(f + \frac{\partial v}{\partial x} - \frac{\partial u}{\partial y} \right)$, $\theta_x = \frac{\partial \theta}{\partial x}$, $\theta_y = \frac{\partial \theta}{\partial y}$, $\theta_z = \frac{\partial \theta}{\partial z}$, $e = 2\Omega \cos \phi$, and $f = 2\Omega \sin \phi$. Variable $\Omega = 7.292 \times 10^{-5} \text{ s}^{-1}$ is the rotation rate of the earth, ϕ is latitude, θ is potential temperature, and α is specific volume.

To evaluate the development of vertical vorticity, taking operator $\frac{D}{Dt}$ on Eq. (3) leads to

$$\begin{aligned} \frac{D\eta_z}{Dt} &= \frac{D}{Dt} \left(\frac{PV_e - PV_2}{\theta_z} \right) \\ &= \frac{1}{\theta_z} \frac{DPV_e}{Dt} - \frac{1}{\theta_z} \frac{DPV_2}{Dt} - \frac{\eta_z}{\theta_z} \frac{D\theta_z}{Dt}, \end{aligned} \quad (5)$$

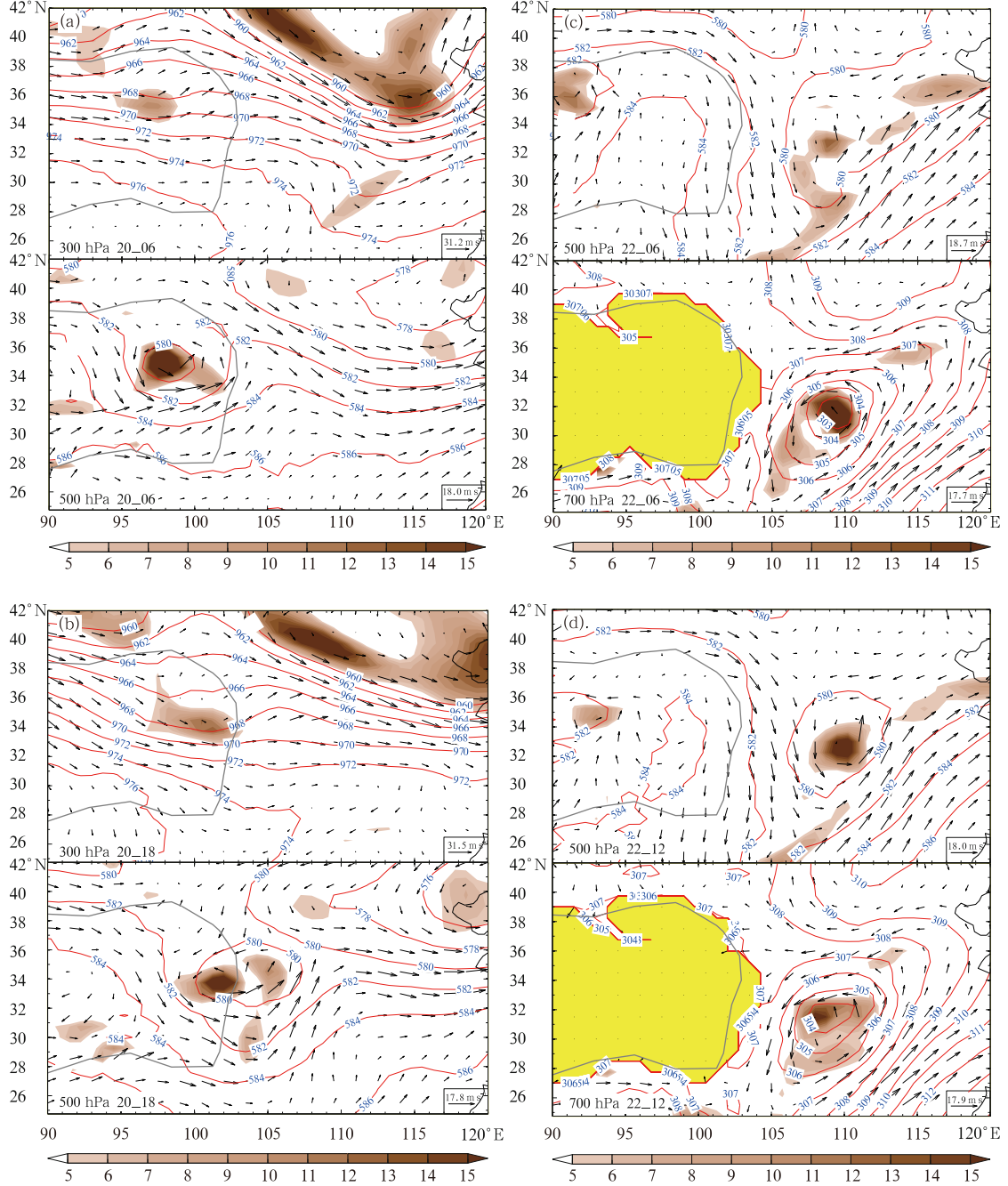


Fig. 3. Distributions of wind (vector), geopotential height (contour; dgpm), and vertical relative vorticity (shading; 10^{-5} s^{-1}) at (a) 300 and 500 hPa at 0600 UTC 20, (b) 300 and 500 hPa at 1800 UTC 20, (c) 500 and 700 hPa at 0600 UTC 22, and (d) 500 and 700 hPa at 1200 UTC 22 July 2008. The yellow masks the region underneath the ground surface, the same for following figures.

where $\frac{D}{Dt} = \frac{\partial}{\partial t} + \mathbf{V} \cdot \nabla$. It demonstrates that the change in PV_e , PV_2 , and θ_z along a Lagrangian particle track can influence the individual change in vertical vorticity of the particle. The second and third terms

on the right hand side of Eq. (5) depend on the atmospheric circulation and thermal configuration, which can be studied through a $PV-\theta$ view (Hoskins, 1991), as will be stressed in the second part of this study.

The first term is determined by static stability θ_z and the change in PV_e :

$$\left(\frac{D\eta_z}{Dt}\right)_Q = \frac{1}{\theta_z} \frac{DPV_e}{Dt}, \quad \theta_z \neq 0. \quad (6)$$

Based on the potential vorticity equation (Ertel, 1942; Hoskins et al., 1985)

$$\frac{DPV_e}{Dt} = \boldsymbol{\eta}_a \cdot \nabla Q + (\alpha \nabla \times \mathbf{F}) \cdot \nabla \theta, \quad (7)$$

where $Q = \frac{D\theta}{Dt}$ denotes diabatic heating, and in the free atmosphere, friction \mathbf{F} can be neglected, then

$$\begin{aligned} \frac{DPV_e}{Dt} &= \boldsymbol{\eta}_a \cdot \nabla Q = \eta_z \frac{\partial Q}{\partial z} + \boldsymbol{\eta}_s \cdot \nabla_s Q \\ &= \left(\frac{DPV_e}{Dt}\right)_z + \left(\frac{DPV_e}{Dt}\right)_s, \end{aligned} \quad (8)$$

where

$$\left\{ \begin{aligned} \left(\frac{DPV_e}{Dt}\right)_z &= \eta_z \frac{\partial Q}{\partial z}, & (9a) \\ \left(\frac{DPV_e}{Dt}\right)_s &= \boldsymbol{\eta}_s \cdot \nabla_s Q, & (9b) \end{aligned} \right.$$

represent the contributions to the PV_e changes due to the non-uniformity of diabatic heating in vertical and horizontal directions, respectively.

3.1 Impacts on vertical vorticity development of the vertical non-uniformity of diabatic heating

In the case of non-uniformity of diabatic heating in vertical direction, according to Eq. (9a), PV_e is increased (decreased) where the vertical gradient of diabatic heating is positive (negative) (Wu and Liu, 2000). This is illustrated schematically in Fig. 4a. In such a circumstance, the vertical gradient of diabatic heating makes positive (negative) PV_e generation below (above) the maximum of the diabatic heating. According to Eq. (6), for a stable stratified atmosphere, the low-level positive PV_e generation corresponds to an increasing cyclonic circulation which can strengthen the low-level vortex, and the upper-level negative PV_e generation corresponds to an increasing anticyclonic circulation which can weaken the upper-level vortex, making the vortex confined in a lower vertical extension.

It should be noted that the condensation diabatic heating in a vortex usually occurs on its eastern side. This is because across the vortex's center, the zonal

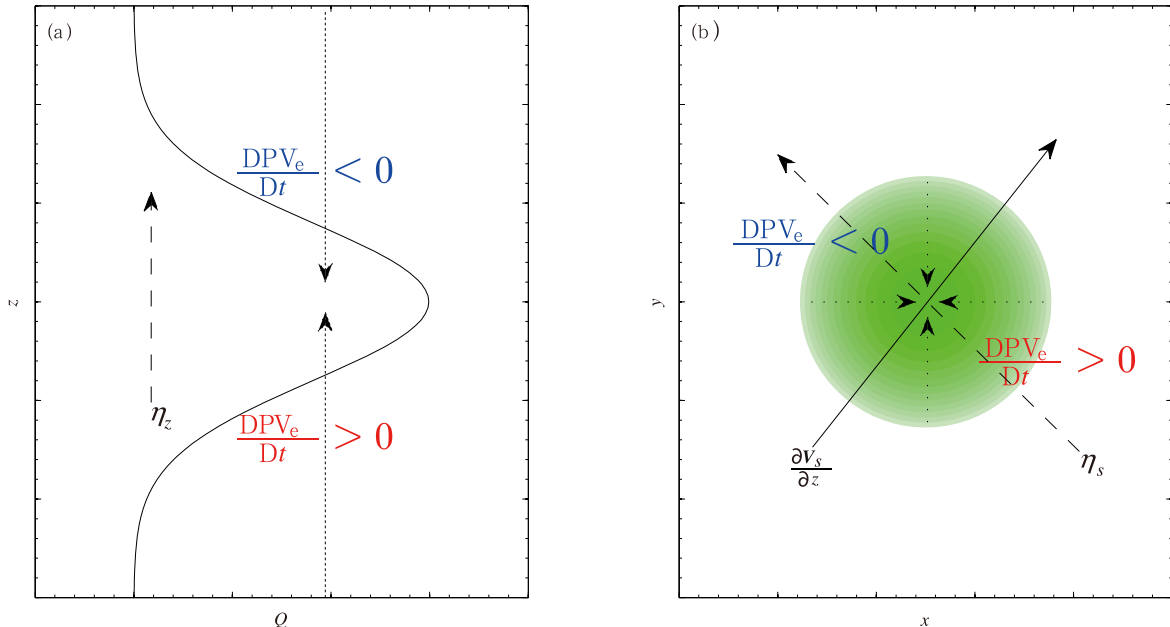


Fig. 4. Lagrangian PV_e generation associated with (a) the vertical profile of diabatic heating Q (thick solid curve), and (b) the horizontal gradient of diabatic heating Q (shading). Long solid arrow is the vertical shear of horizontal wind ($\frac{\partial V_s}{\partial z}$), long dashed arrow in (a) is the vertical vorticity η_z and in (b) is the horizontal vorticity η_s , and short dot arrows in (a) are the vertical gradient of diabatic heating $\frac{\partial Q}{\partial z}$ and in (b) are $\nabla_s Q$, which is the horizontal gradient of diabatic heating Q .

advection of vorticity is negligible. Consequently, the vorticity equation at a steady state can be approximated as $\beta v \simeq f \frac{\partial w}{\partial z}$ and the vertical velocity becomes $w \propto -\frac{\beta}{f} \frac{\partial v}{\partial z}$. Since on the eastern (western) side of a vortex, $\frac{\partial v}{\partial z} < 0$ ($\frac{\partial v}{\partial z} > 0$), air rising (sinking) occurs normally on the eastern (western) side of the vortex. This implies that condensation diabatic heating usually occurs on the eastern side of a vortex. Consequently, the generation of positive vorticity in the lower troposphere on the east of a vortex associated with the vertical non-uniformity of condensation diabatic heating will contribute to the eastward movement of the vortex.

3.2 Impacts on vertical vorticity development of the horizontal non-uniformity of diabatic heating

According to Eq. (9b), the horizontal gradient of diabatic heating may contribute to the development of the vertical vorticity of a vortex: there is positive (negative) potential vorticity generation when the horizontal vorticity $\boldsymbol{\eta}_s$ and the horizontal gradient $\boldsymbol{\theta}_s$ of diabatic heating are in the same (opposite) direction, i.e., the potential vorticity generation is maximum (zero) when two vectors are coincided (orthogonal). As the horizontal variation of vertical velocity w is several orders less than the vertical shear of horizontal wind \mathbf{V}_s , Eq. (9b) is approximated as

$$\left(\frac{DPV_e}{Dt}\right)_s = \boldsymbol{\eta}_s \cdot \nabla_s Q \simeq \alpha \left(\mathbf{k} \times \frac{\partial \mathbf{V}_s}{\partial z}\right) \cdot \nabla_s Q. \quad (10)$$

This means that the sign of the change of PV_e depends on the disposition between the atmosphere circulation and diabatic heating. As schematically illustrated in Fig. 4b, because the vertical shear of horizontal wind ($\frac{\partial \mathbf{V}_s}{\partial z}$) corresponds to horizontal vorticity ($\boldsymbol{\eta}_s$) with its direction perpendicular to, and pointing to the left of the shear vector in the Northern Hemisphere, and because the direction of the horizontal gradient of diabatic heating ($\nabla_s Q$) points towards the center of the diabatic heating, consequently on the right (left) side of the shear vector, the scalar product of horizontal vorticity ($\boldsymbol{\eta}_s$) associated with the vertical shear of hori-

zontal wind ($\frac{\partial \mathbf{V}_s}{\partial z}$) and the horizontal gradient of diabatic heating ($\nabla_s Q$), i.e., $\boldsymbol{\eta}_s \cdot \nabla_s Q$, is positive (negative), and positive (negative) PV_e generation is on the right (left) side of the shear vector. According to Eq. (6), in a stable stratified atmosphere, positive and negative vorticities will be generated, respectively, on the right and left sides of the vertical shear of horizontal wind. In such a circumstance, the horizontal gradient of diabatic heating can not only strengthen the vertical vorticity on the right side of the shear vector and weaken the vertical vorticity on the left side of the shear vector, but also further influence the movement of the vortex since the tendency of vertical vorticity generation is asymmetrically distributed on the two sides of the shear vector which passes through the center of diabatic heating, which is usually on the eastern side of the vortex.

4. PV–Q view on the development and movement of the TPV

The above study is based on a Lagrangian perspective. For application to the TPV in July 2008 based on the ERA-Interim reanalysis with a time span of 6 h, we need to conduct a Lagrangian scheme for the corresponding diagnosis. The Lagrangian change of any quantity q can be evaluated as:

$$\frac{Dq}{Dt} = \frac{q(\mathbf{r}(t)) - q(\mathbf{r}(t - \Delta t))}{\Delta t}, \quad (11)$$

where $\mathbf{r}(t)$ and $\mathbf{r}(t - \Delta t)$ are the arrival position and departure position of a particle, respectively. The standard iterative algorithm for backward trajectory in Semi-Lagrangian transport scheme is not accurate enough for very large time step. Here, the large time step is divided into multismall intervals, in each small interval $\delta\tau$, the departure position $\mathbf{r}(\tau - \delta\tau)$ can be obtained by Taylor series expansion of $\mathbf{r}(\tau - \delta\tau)$ about the arrival position $\mathbf{r}(\tau)$ following the idea of McGregor (1993):

$$\mathbf{r}(\tau - \delta\tau) = \mathbf{r}(\tau) + \sum_{n=1}^N \frac{(-\delta\tau)^n}{n!} \frac{D^n \mathbf{r}(\tau)}{D\tau^n} + O(\delta\tau^{N+1}). \quad (12)$$

In Cartesian coordinates, $\mathbf{r}(\tau) = r \cos \lambda \cos \phi \mathbf{i} +$

$r \sin \lambda \cos \phi \mathbf{j} + r \sin \phi \mathbf{k}$, then the first derivative $\frac{D\mathbf{r}(\tau)}{D\tau}$ required in Eq. (12) is calculated analytically as

$$\begin{aligned} \frac{D\mathbf{r}(\tau)}{D\tau} = & [-u \sin \lambda - v \cos \lambda \sin \phi + w \cos \lambda \cos \phi] \mathbf{i} \\ & + [u \cos \lambda - v \sin \lambda \sin \phi + w \sin \lambda \cos \phi] \mathbf{j} \\ & + [v \cos \phi + w \sin \phi] \mathbf{k}. \end{aligned} \quad (13)$$

By taking $\frac{D}{D\tau}$ on Eq. (13) and dropping the higher-order terms $\frac{D^2\lambda}{D\tau^2}$, $\frac{D^2\phi}{D\tau^2}$, and $\frac{D^2r}{D\tau^2}$, the second derivative $\frac{D^2\mathbf{r}(\tau)}{D\tau^2}$ required in Eq. (12) is approximated as

$$\begin{aligned} \frac{D^2\mathbf{r}(\tau)}{D\tau^2} \simeq & \left[-2\frac{uw}{r} \sin \lambda - 2\frac{vw}{r} \cos \lambda \sin \phi \right. \\ & + 2\frac{uv}{r} \sin \lambda \tan \phi - \frac{u^2}{r \cos \phi} \cos \lambda \\ & \left. - \frac{v^2}{r} \cos \lambda \cos \phi \right] \mathbf{i} + \left[2\frac{uw}{r} \cos \lambda \right. \\ & \left. - 2\frac{vw}{r} \sin \lambda \sin \phi - 2\frac{uv}{r} \cos \lambda \tan \phi \right. \\ & \left. - \frac{u^2}{r \cos \phi} \sin \lambda - \frac{v^2}{r} \sin \lambda \cos \phi \right] \mathbf{j} \\ & + \left[2\frac{vw}{r} \cos \phi - \frac{v^2}{r} \sin \phi \right] \mathbf{k}. \end{aligned} \quad (14)$$

Since the derivatives $\frac{D\mathbf{r}(\tau)}{D\tau}$ and $\frac{D^2\mathbf{r}(\tau)}{D\tau^2}$ are obtained analytically, the algorithm Eq. (12) is at a third order precision and is more accurate than the numerical iterative algorithm. Therefore, Eq. (11) is adopted for calculating the Lagrangian change of various variables in the following study.

4.1 Relative contributions to vertical vorticity development of the changes in PV_e , PV_2 , and θ_z

By employing Eq. (11) to each term in Eq. (5), the change in vertical vorticity is calculated for every time step. Figure 5 shows these relative contributions when the vortex slides down the TP, i.e., the relative contributions to the development of vertical vorticity, respectively, due to the change in PV_e , PV_2 , and θ_z . It is demonstrated that the contribution due to the change of PV_e $\left(\frac{1}{\theta_z} \frac{DPV_e}{Dt}\right)$ is analogous to the total change of the vertical vorticity $\left(\frac{D\eta_z}{Dt}\right)$ with the same

order of magnitudes. The positive center of the contribution due to the change in PV_2 $\left(-\frac{1}{\theta_z} \frac{DPV_2}{Dt}\right)$ is coincident with the development center of vertical vorticity of TPV, though weaker in magnitude compared to the diabatic heating impact. On the other hand, the contribution due to the change of static stability θ_z to the development of vertical vorticity $\left(-\frac{\eta_z}{\theta_z} \frac{D\theta_z}{Dt}\right)$ is usually negative and is weaker in magnitude, i.e., the vertical vorticity decreases when the static stability θ_z increases. In other words, in a stable atmosphere, when the atmosphere becomes more stable, it is not favorable for the development of vortex. This differs from the linear model of the flow over mountain (on the lee side, the air column is stretched and the static stability θ_z decreases, and then the vertical vorticity develops). The increasing in θ_z is due to the nonlinear effect of the flow around the TP and the diabatic heating, that is, the decreasing of elevation and nocturnal surface cooling weaken low-level heating, and mid-level condensation latent heating associated with precipitation increases θ_z , so the Lagrangian change of θ_z increases. The above analysis indicates that the Lagrangian change of PV_e associated with diabatic heating plays a leading role in the development of vertical vorticity during the severe development of the TPV.

During the second stage of the TPV development, at 0000 UTC 22 July 2008 (Fig. 6a), the vertical vorticity developed at low level near 700 hPa, and weakened at middle level near 500 hPa. At 0600 UTC (Fig. 6b), the vertical vorticity intensified at both low and middle levels and the TPV reached above 500 hPa. At 1200 UTC (Fig. 6c), the development of vertical vorticity near 500 hPa maintained but that at 700 hPa began to weaken. Afterwards, the vertical vorticity at both low and middle levels weakened and moved northeastward gradually (figure omitted). The same pattern can be seen more clearly from the contribution due to the change of PV_e (second column in Fig. 6). In addition, it can be seen that the contribution due to the change of the horizontal component PV_2 of PV_e was also significant near 500 hPa at 0600 UTC (Fig. 6b). As in the first stage, the contribution due to the change of static stability θ_z was negative at 0000 UTC

20 July 2008 (Fig. 6a). But it can be seen from Figs. 6b and 6c that the contribution due to the change of static stability θ_z was positive surrounding the vortex's center. This means that in such circumstances, the static stability θ_z contributes positively to the development of vertical vorticity, i.e., when the static stability θ_z decreases (increases) in a stable (unstable) atmosphere, the vertical vorticity will develop.

4.2 Effect of the vertical gradient of diabatic heating

The above results demonstrate that the change of PV_e plays a leading role in the development of vertical vorticity. The change of PV_e is due to friction and diabatic heating. According to Eq. (9a), in the free atmosphere, the change of PV_e is due to diabatic

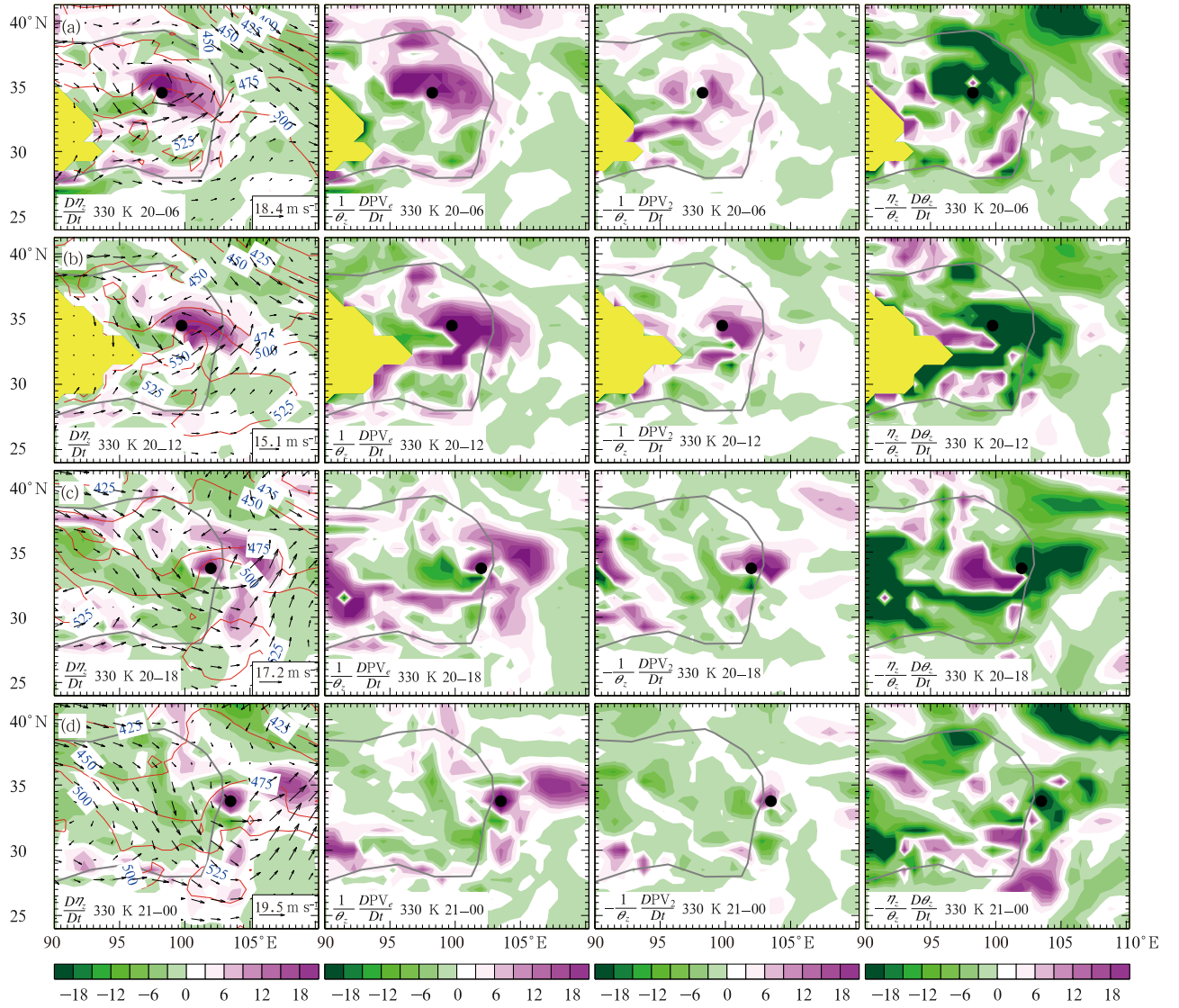


Fig. 5. Relative contributions of the changes in PV_e , PV_2 , and θ_z to the development of vertical vorticity η_z on the 330-K isentropic surface at (a) 0600 UTC 20, (b) 1200 UTC 20, (c) 1800 UTC 20, and (d) 0000 UTC 21 July 2008. The contour line is pressure in hPa, the vector is horizontal wind, and the shading ($10^{-5} \text{ m}^3 (\text{kg s } 6 \text{ h})^{-1}$) in the first column is the change of vertical vorticity η_z , those in the second, third, and fourth columns are the contributions to the development of vertical vorticity due to the changes of PV_e , PV_2 , and θ_z , respectively. The black solid circles are the locations of the TPV, the same for following figures.

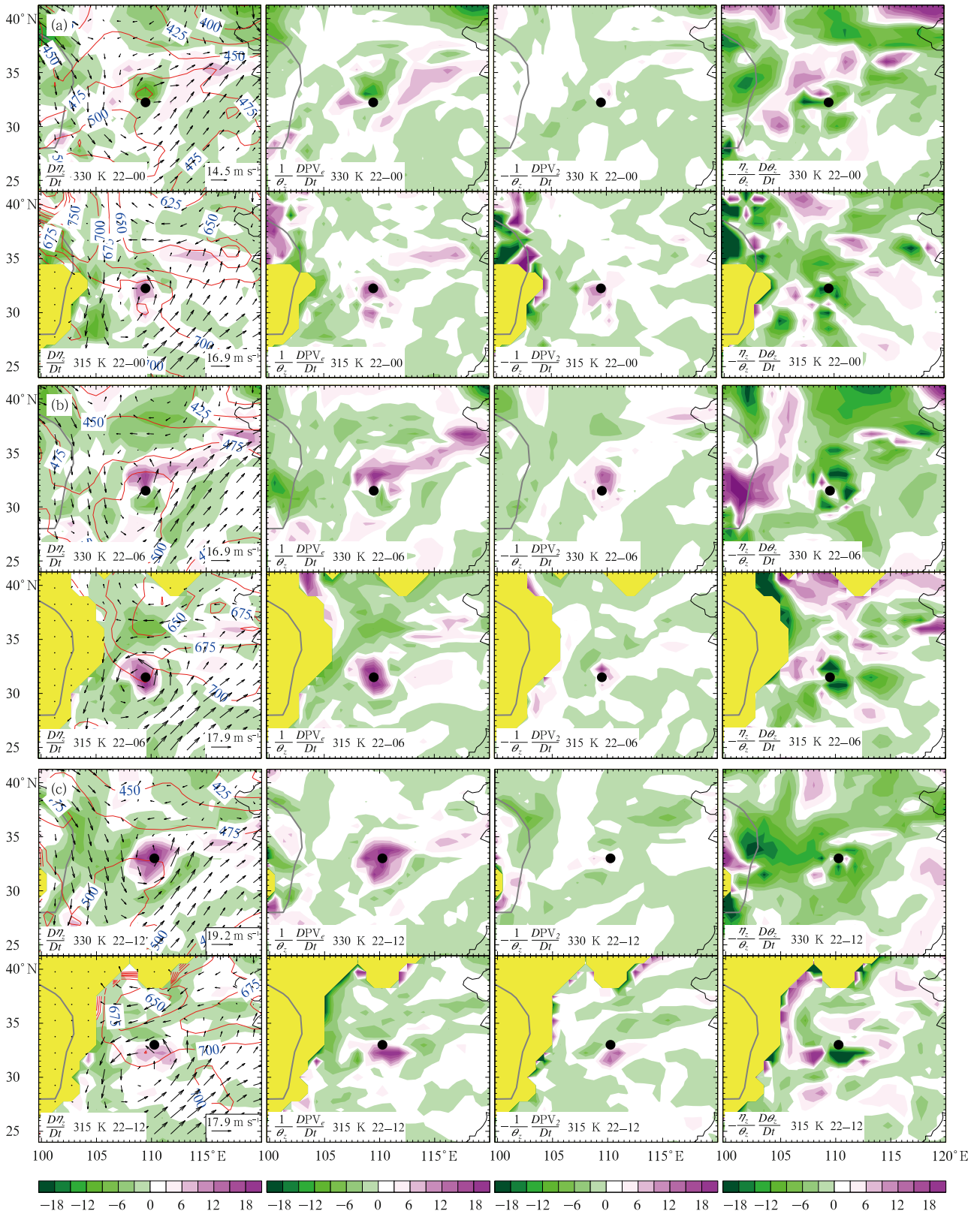


Fig. 6. As in Fig. 5, but on the 330- and 315-K isentropic surfaces at (a) 0000, (b) 0600, and (c) 1200 UTC 22 July 2008.

heating. To understand its impact, the total change in vertical vorticity η_z , the change in PV_e , the diabatic heating Q , and the effect of the vertical gradient of diabatic heating ($\eta_z \frac{\partial Q}{\partial z}$) for the second period are demonstrated in Fig. 7.

At 1800 UTC 21 July 2008, there was no significant diabatic heating at middle level, the low-level positive PV_e generation made by the vertical gradient of diabatic heating was weak, so the development of the low level vortex was weak and the TPV concen-

trated at low level (figure omitted). Afterwards, when the TPV arrived at the up-slope of the northeastern edge of the Sichuan basin, the diabatic heating got strengthened and uplifted gradually from 0000 to 1200 UTC 22 July 2008 (Fig. 7). Correspondingly, the vertical vorticity in the lower troposphere near the vortex center was intensified, and the TPV developed vertically above 500 hPa, which is consistent with those presented in Figs. 3c, 3d, and 6. It clearly shows that there was positive PV_e generation below the maximum

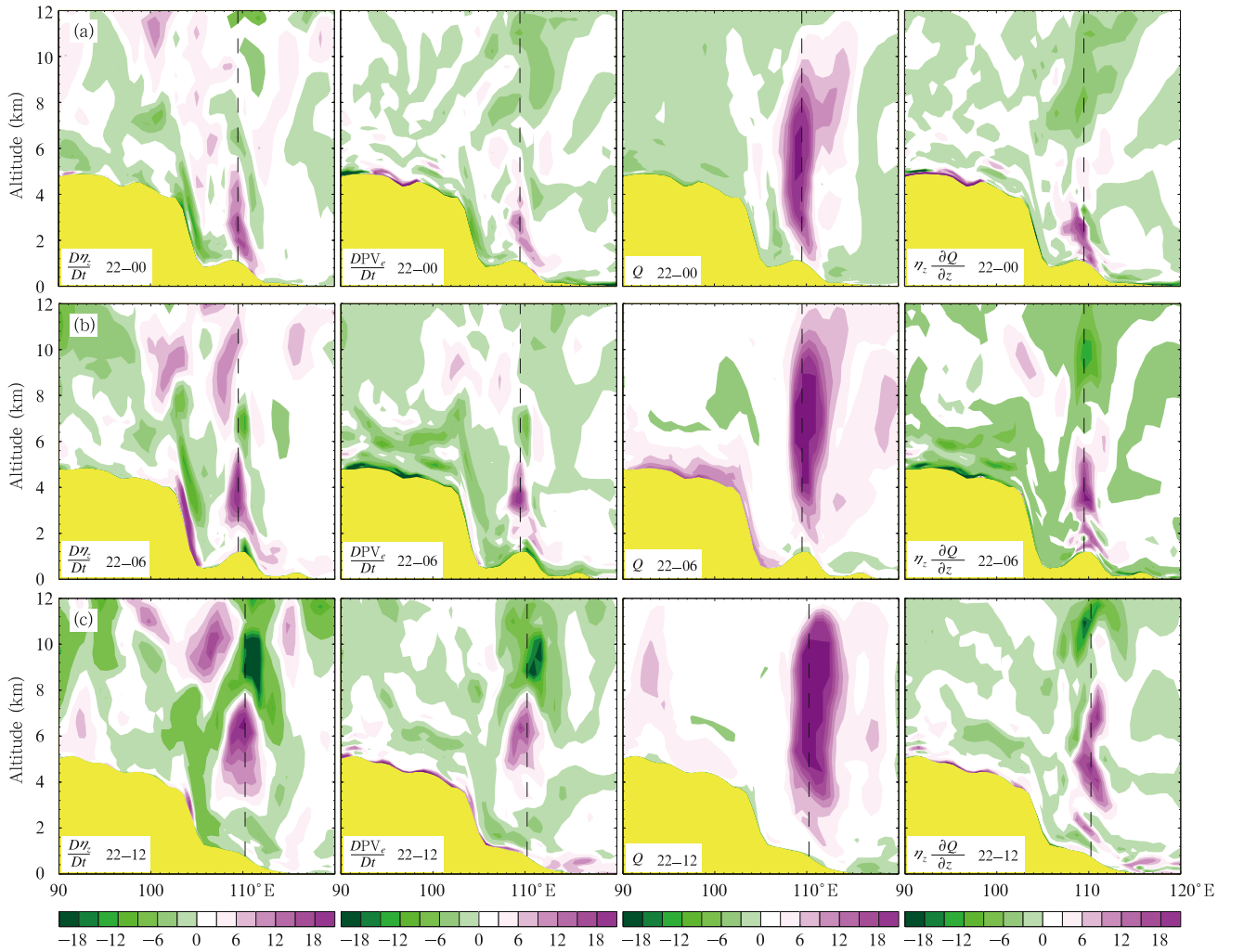


Fig. 7. Zonal vertical cross-sections across the center of the TPV at (a) 0000, (b) 0600, and (c) 1200 UTC 22 July 2008. The vertical dashed line denotes the location of the center of TPV. The shadings in the first, second, third, and fourth columns are, respectively, the Lagrangian change of vertical vorticity η_z ($\frac{D\eta_z}{Dt}$; $10^{-5} \text{ m}^3 (\text{kg s}^6 \text{ h})^{-1}$), the Lagrangian change of Ertel potential vorticity PV_e ($\frac{DPV_e}{Dt}$; $10^{-1} \text{ PVU} (6 \text{ h})^{-1}$), the diabatic heating Q ($\text{K} (6 \text{ h})^{-1}$), and the change of PV_e due to the vertical gradient of diabatic heating ($\eta_z \frac{\partial Q}{\partial z}$; $10^{-1} \text{ PVU} (6 \text{ h})^{-1}$).

of diabatic heating to strengthen the low-level vortex and negative PV_e generation above it to weaken the upper-level vortex.

4.3 Effect of the horizontal gradient of diabatic heating

It is worthwhile to note that in Fig. 7, there is distinct differences between $\frac{DPV_e}{Dt}$ and $\eta_z \frac{\partial Q}{\partial z}$. This implies that other factors, such as the horizontal gradient of diabatic heating, also contribute to the development of vertical vorticity under certain circumstances.

In different development stages of the TPV, the distributions of $\eta_s \cdot \nabla_s Q$, the diabatic heating Q , and the vertical shear of horizontal wind $\frac{\partial \mathbf{V}_s}{\partial z}$ are shown in Figs. 8 and 9. According to Eq. (9b), the positive PV_e generation in association with the intensification of vertical vorticity, i.e., $\left(\frac{DPV_e}{Dt}\right) = \eta_s \cdot \nabla_s Q$, is mostly located on the right side of the vertical shear of horizontal wind $\left(\frac{\partial \mathbf{V}_s}{\partial z}\right)$ across the center of the diabatic heating. Although the magnitude of the PV_e generation due to the horizontal gradient of diabatic heating is commonly one order of magnitude less than that due to vertical gradient of diabatic heating, sometimes it can reach the same order. Such a case happened after the vortex slid down the TP at 0600 UTC

21 July 2008 (Fig. 8c) and when it was climbing up the hillside over northern Sichuan basin at 0600 UTC 22 July 2008 (Fig. 9b). It is evident from the figures that the movement of the vortex was toward the positive PV_e generation on the right side of vertical shear of horizontal wind at 400 hPa due to the horizontal gradient of diabatic heating in most cases. For example, the suddenly southward shift of the vortex's track at 1200 UTC 21 July 2008 (Fig. 8d) was well correlated with the fact that the positive PV_e generation associate with the horizontal gradient of diabatic heating was located to its south. There was an exception at 1200 UTC 22 July 2008 (Fig. 9c) when the vortex had climbed up the hill and became weaker and stagnant over it (Fig. 2). Even so, the maximum of $\eta_s \cdot \nabla_s Q$ at that moment was still on the eastern side of the TPV, leading to the eastward movement of the vortex afterwards. The relationship between the movement of TPV and the positive PV_e generation due to the horizontal gradient of diabatic heating was most obvious at 400 hPa than other levels (figure omitted).

5. Conclusions and discussion

Based on the Lagrangian change equation of vertical vorticity deduced from the equation of three-

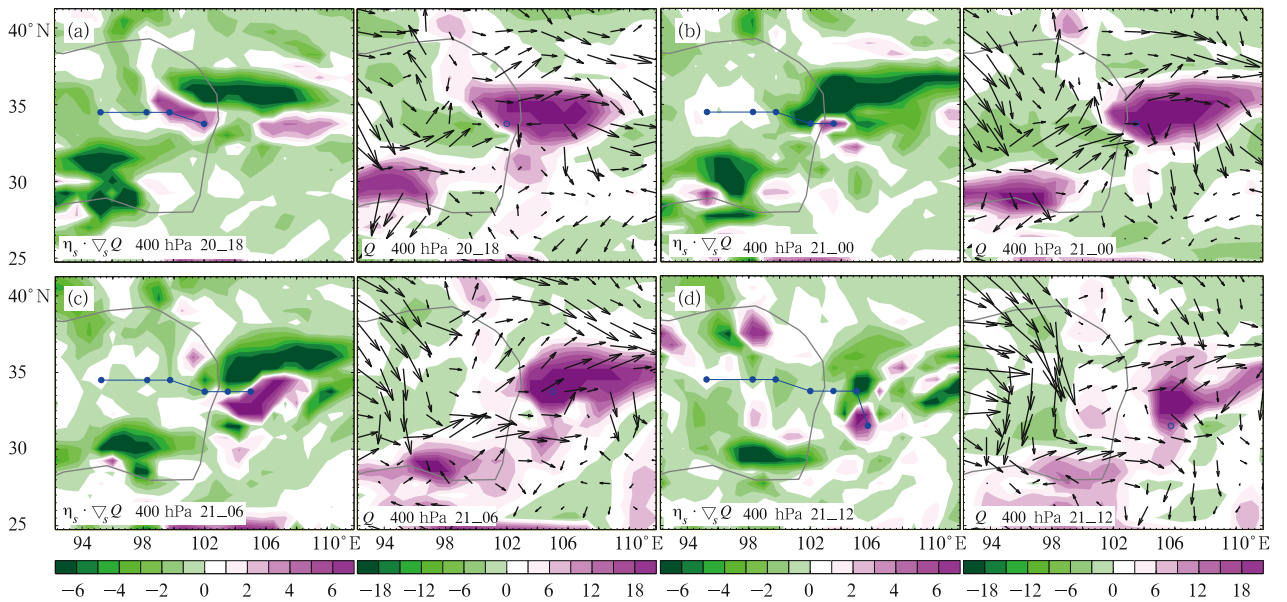


Fig. 8. The Lagrangian change of PV_e (first column; $5 \times 10^{-2} \text{ PVU} (6 \text{ h})^{-1}$) due to the horizontal gradient of diabatic heating (second column; $5 \times 10^{-1} \text{ K} (6 \text{ h})^{-1}$) at 400 hPa at (a) 1800 UTC 20, (b) 0000 UTC 21, (c) 0600 UTC 21, and (d) 1200 UTC 21 July 2008. The vector denotes vertical shear of horizontal wind.

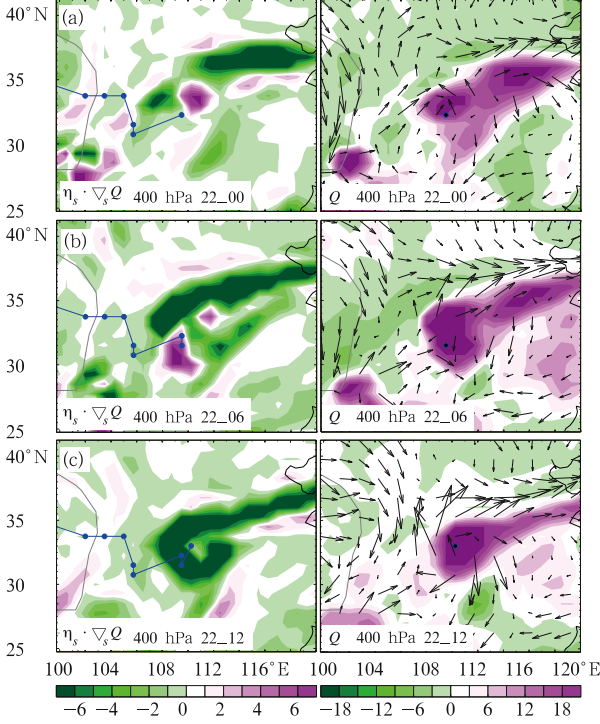


Fig. 9. As in Fig. 8, but at (a) 0000, (b) 0600, and (c) 1200 UTC 22 July 2008.

dimensional PV_e , the development and movement of vortex are studied from a $PV-Q$ perspective. The theory just developed are employed to diagnose the development and movement of a TPV that occurred in July 2008.

The relative contribution to the development of vertical vorticity due to the change in Ertel potential vorticity PV_e , the horizontal component PV_2 , and the static stability θ_z are analyzed by employing the ERA-Interim reanalysis data. It is demonstrated that in static stable atmosphere, the Lagrangian change of PV_e associated with diabatic heating of condensation plays a leading role; the change of horizontal component PV_2 has positive but less significant contribution; and the change of static stability θ_z usually has a negative effect on the development of vertical vorticity in a stable atmosphere as the atmosphere becomes more stable. But surrounding the vortex's center, the vertical vorticity develops rapidly as the static stability θ_z decreases (increases) in the stable (unstable) atmosphere. These indicate that strong stable and strong unstable conditions are not favorable for the development of vortex, while near neutral stratification

is favorable for the development of vortex, i.e., the vertical vorticity will develop rapidly when the static stability θ_z approaches zero. The difference between the effect of the change in θ_z and the linear model of the flow over mountain is mainly due to the nonlinear effect of flow around the TP and diabatic heating.

The role of diabatic heating in the vortex's development and movement is investigated in much detail. The vertical gradient of the diabatic heating makes positive PV_e generation that strengthens the vertical vorticity below the maximum of diabatic heating, and makes negative PV_e generation that weakens the vertical vorticity above the maximum of diabatic heating. It is shown that the re-intensification of the TPV whose vertical extent reaches above 500 hPa again during its second stage is mainly due to the re-strengthening and the vertical uplifting of the diabatic heating. Because condensation heating usually occurs on the eastern side of a vortex, the effect of the vertical non-uniformity heating is to move the vortex eastward besides to intensify the local vertical vorticity. The horizontal gradient of diabatic heating makes positive PV_e generation on the right side of the vertical shear of horizontal wind, and negative PV_e generation on the left side. The positive PV_e generation not only intensifies the vertical vorticity on the right side of the vertical shear of horizontal wind, but also leads to the movement of the vortex towards the positive generation site.

It should be pointed out that though the above conclusions are demonstrated merely by one case, they are reliable since they can be explained mathematically by the theory of Lagrangian change equation of vertical vorticity, and the relationship between the horizontal movement and the horizontal gradient of diabatic heating and its robustness needs more cases for verification. Also, the formation of TPV, which is not touched in this paper, is an interesting topic that is worthy a thorough investigation.

REFERENCES

- Chen Bomin, Qian Zhengan, and Zhang Lisheng, 1996: Numerical simulation of the formation and development of vortices over the Qinghai-Xizang Plateau

- in summer. *Scientia Atmospherica Sinica*, **20**, 491–502. (in Chinese)
- Chen Zhongming, Min Wenbin, Xu Maoliang, et al., 2004: Mesoscale characteristics of the unbalanced force of atmospheric motion and environmental fields of rain storm on 20–21 July 1998. *Acta Meteor. Sinica*, **62**, 375–383. (in Chinese)
- Cui Xiaopeng, Wu Guoxiong, and Gao Shouting, 2002: Numerical simulation and isentropic analysis of frontal cyclones over the western Atlantic Ocean. *Acta Meteor. Sinica*, **60**, 385–399. (in Chinese)
- Dee, D. P., S. M. Uppala, A. J. Simmons, et al., 2011: The ERA-Interim reanalysis: Configuration and performance of the data assimilation system. *Quart. J. Roy. Meteor. Soc.*, **137**, 553–597.
- Ding Yihui, 1993: *Monsoons over China*. Springer, 432 pp.
- , 2005: *Advanced Synoptic Meteorology*. China Meteorological Press, Beijing, 585 pp. (in Chinese)
- Ding Zhiying and Lu Junyu, 1990: A numerical experiment on the eastward movement of a Qinghai-Xizang Plateau vortex. *J. Nanjing Institute of Meteorology*, **13**, 426–433. (in Chinese)
- Ertel, H., 1942: Ein neuer hydrodynamische wirbdsatz. *Meteorology Z. Braunschweig*, **59**, 33–49.
- Group of Tibetan Plateau Low Value System, 1978: The preliminary research on the formation and development of the Tibetan Plateau vortex in boreal summer. *Sci. China (Ser. A)*, **3**, 341–350.
- Hoskins, B., 1991: Towards a PV- θ view of the general circulation. *Tellus*, **43AB**, 27–35.
- , M. McIntyre, and A. Robertson, 1985: On the use and significance of isentropic potential vorticity maps. *Quart. J. Roy. Meteor. Soc.*, **111**, 877–946.
- Huffman, G., R. Adler, D. Bolvin, et al., 2007: The TRMM multi-satellite precipitation analysis: Quasi-global, multi-year, combined-sensor precipitation estimates at fine scale. *J. Hydrometeor.*, **8**, 38–55.
- Jiang Yongqiang, Chen Zhongyi, Zhou Zugang, et al., 2004: Slantwise vorticity development and meso- β scale low vortex. *Journal of PLA University of Science and Technology*, **5**, 81–87. (in Chinese)
- Li Guoping, 2002: *The Tibetan Plateau Dynamic Meteorology*. China Meteorological Press, Beijing, 271 pp. (in Chinese)
- Liu Fuming and Fu Meijuan, 1985: A study on the eastward moving lows over Qinghai-Xizang Plateau. *Plateau Meteorology*, **5**, 125–134. (in Chinese)
- Ma Leiming, Qin Zengying, Duan Yihong, et al., 2002: Case study on the impact of atmospheric baroclinicity to the initial development of Jianghuai cyclones. *Acta Oceanologica Sinica*, **24**, 95–104.
- McGregor, J., 1993: Economical determination of the departure points for the Semi-Lagrangian models. *Mon. Wea. Rev.*, **121**, 221–230.
- Qiao Quanming, 1987: The environment analysis on 500-hPa vortexes moving eastward out of Tibetan Plateau in summer. *Plateau Meteorology*, **6**, 45–55. (in Chinese)
- and Zhang Yagao, 1994: *Synoptic Meteorology of the Tibetan Plateau*. China Meteorological Press, Beijing, 250 pp. (in Chinese)
- Shen, R., E. Reiter, and J. Bresch, 1986: Numerical simulation of the development of vortices over the Qinghai-Xizang (Tibet) Plateau. *Meteor. Atmos. Phys.*, **35**, 70–95.
- Sun Guowu and Chen Baode, 1988: Dynamic processes of the moving and development low on the Qinghai-Xizang Plateau during the early summer. *Journal of Academy of Meteorological Sciences*, **3**, 56–63.
- Tao Shiyan, 1980: *Chinese Rainstorms*. Science Press, Beijing, 226 pp. (in Chinese)
- , and Y. Ding, 1981: Observational evidence of the influence of the Qinghai-Xizang (Tibet) Plateau on the occurrence of heavy rain and severe convective storms in China. *Bull. Amer. Meteor. Soc.*, **62**, 23–30.
- Wang Ying, Wang Yuan, Zhang Lixiang, et al., 2007: The development of slantwise vorticity near a weakened tropical cyclone. *Journal of Tropical Meteorology*, **23**, 47–52. (in Chinese)
- Wu, G., and H. Liu, 1997: Vertical vorticity development owing to down-sliding at slantwise isentropic surface. *Dyn. Atmos. Ocean.*, **27**, 715–743.
- Wu Guoxiong and Liu Yimin, 2000: Thermal adaptation, overshooting, dispersion, and subtropical anticyclone. Part I: Thermal adaptation and overshooting. *Chinese J. Atmos. Sci.*, **24**, 433–446. (in Chinese)
- Ye Duzheng and Gao Youxi, 1979: *The Tibetan Plateau Meteorology*. Science Press, Beijing, 316 pp. (in Chinese)
- Zhang Jijia, Zhu Baozhen, and Zhu Fukang, 1988: *Tibetan Plateau Meteorological Progresses*. Science Press, Beijing, 432 pp. (in Chinese)